Published in final edited form as:
*Biochemistry*. 2008 December 9; 47(49): 13046–13055. doi:10.1021/bi8012559.

# Methodology to probe subunit interactions in ribonucleotide reductases†

**A Quamrul Hassan**‡, **Yongting Wang**§,⊥, **Lars Plate**‡, and **JoAnne Stubbe***,§,‡
*Departments of Chemistry and Biology, Massachusetts Institute of Technology, Cambridge MA 02139.*

‡*Department of Chemistry, Massachusetts Institute of Technology.*

§*Department of Biology ( Present address), Massachusetts Institute of Technology.*

## Abstract

Ribonucleotide reductases (RNRs) catalyze the conversion of nucleotides to deoxynucleotides, providing the monomeric precursors required for DNA replication and repair. *E. coli* RNR is a 1:1 complex of two homodimeric subunits: α2 and β2. The interactions between α2 and β2 are thought to be largely associated with the C-terminal 20 amino acids (residues 356-375) of β2. To study subunit interactions, a single reactive cysteine has been introduced into each of fifteen positions along the C-terminal tail of β2. Each cysteine has been modified with the photo cross-linker benzophenone (BP) and the environmentally sensitive fluorophore, dimethylaminonaphthalene (DAN). Each construct has been purified to homogeneity and characterized by SDS PAGE and ESI-MS. Each BP-β2 has been incubated with 1 equivalent of α2, photolyzed, and the results analyzed quantitatively by SDS-PAGE. Each DAN-β2 was incubated with 50-fold excess of α2 and the emission maximum and intensity measured. A comparison of the results from the two sets of probes reveals that sites with most extensive cross-linking are also associated with the greatest changes in fluorescence. Titration of four different DAN-β2 variants (351, 356, 365 and 367) with α2 gave a $K_d$ of ~0.4 μM for subunit interaction. Disruption of the interaction of α2DAN-β2 complex is accompanied by a decrease in fluorescence intensity and can serve as a high throughput screen for inhibitors of subunit interactions.

Ribonucleotide reductases (RNRs) catalyze the conversion of nucleoside-5′-di or triphosphates (NDPs or NTPs) to deoxynucleoside-5′-di- or tri-phosphates (dNDPs or dNTPs) in all organisms, and thus provide the essential precursors for DNA replication and repair(1,2). In *E. coli*, the active RNR is a 1:1 complex (α2β2) of two homodimeric subunits(3-5). The α2 subunit binds both NDP substrates, and the dNTP/ATP allosteric effectors that govern the specificity and rate of dNDP production. The β2 subunit houses the diferric tyrosyl radical (Y•) cofactor (6,7) that is required to initiate the nucleotide reduction on α2, 35 Å μremoved(8). No structure of an active $\alpha_n\beta_n$ complex of any class Ia RNR is available(9). Thus, the molecular details of subunit interactions essential for understanding radical propagation across the subunit

†This work was supported by the NIH grant (GM29595 to J.S.). A Quamrul Hassan is an Anna Fuller fellow funded by David H. Koch Institute for Integrative Cancer Research at MIT.

*To whom correspondence should be addressed. Tel: (617) 253-1814. Fax: (617) 258-7247. E-mail: stubbe@mit.edu.
⊥Present address Department of Biology, Massachusetts Institute of Technology.

**Supporting information available.** The following supporting information is available free of charge via the Internet at http://pubs.acs.org: List of primers used for mutagenesis experiments (Table 1.), the purification yield and radical content of β2 mutants (Table 2.), ESI-MS data for BP-β2 variants (Table 3), ESI-MS data for DAN-β2 variants (Table 4), the relative extent of photo cross-linking of BP-β2 variants (Table 5), fluorescence intensities and emission maxima of DAN-β2 variants (Table 6), residues on α2 interacting with peptide 356-375 equivalent to the C-terminal tail of β2 (Table 7), ESI-MS spectrum for BP-β2 (V365C) (Figure 1).

interface and allosteric regulation that triggers this propagation remains an important issue to resolve. This paper describes new methodology to gain insight about this interface.

Several structures of α2 and of β2 are available (8,10-13) however, and have provided a framework for methodology design. *E. coli* α2 (761 residues) in complex with a peptide composed of residues 356-375 of the C-terminus of β2 (*E. coli* β2 has 375 amino acids) was crystallized and solved. In this structure, residues 358-375 of the peptide were visible(8,13). The binding mode of this peptide was proposed to be indicative of how C-terminal tail of β2 binds to α2. Many structures of *E. coli* β2 are also available. In all cases, only residues 1-340 are visible(11,12), with the remaining 35 residues, including 358-375, being disordered. Thus, no structural information is yet available about residues 341-357 of β2 and their roles in mediating subunit interactions.

Based on the individual structures of α2 and β2, Eklund and coworkers generated a docking model of a 1:1 complex of α2β2 using shape complimentarily and charge compatibility(8). The model is the basis for the 35 Å distance proposed between the essential Y• ($Y_{122}$) in β2 and the active site cysteine ($C_{439}$) in α2. Recent pulsed electron-electron double resonance experiments support this long distance and the docking model(14,15). An independent validation of the model through identification of α2β2 interaction sites is required to increase our understanding of this unique long-range radical transfer pathway and its control by allosteric effectors.

## β is an obligate dimer (β2), while α is an equilibrium mixture of monomer and dimer (α2) with the dimer predominating in the presence of nucleotide (3)

Interactions between α2 and β2 in all class I RNRs thus far examined are weak and largely dependent on the C-terminal 10-20 amino acids of β2 (16-18). The weak interaction, the potential changes in this interaction in the presence of substrates and/or allosteric effectors that bind to α2, and the consequences of these changes on enzymatic activity have prompted a number of studies to determine the $K_d$s for subunit interaction (19-21). Early studies used sucrose gradient ultracentrifugation and showed that allosteric effectors are required in the gradient for detection of α2β2 complex formation(4). Inhibition studies with α2, β2, CDP and ATP monitoring rate of dNDP formation using inactive β2 (Y122F) or using peptides of varying length corresponding to C-terminus of β2, revealed a $K_m$ of 0.2 μM for α2 and β2 (18,21). Recently, surface plasmon resonance techniques were examined in an effort to determine the influence of allosteric effectors and/or substrates on subunit affinity (20). Unfortunately, technical problems in attaching β2 to the sensor chips have limited data interpretation. Thus, there is a gap in our quantitative understanding of complex formation between the subunits. Such information may well be important for the development of a quantitative description of allosteric regulation in class Ia RNRs in general and *E. coli* RNR specifically.

In the present paper, development of a method to probe subunit interactions is reported in which all surface reactive cysteines in β2 are removed and a single cysteine has been incorporated site-specifically into 15 positions in its C-terminal tail. Each cysteine mutant has been modified with the photo cross-linker benzophenone (BP) to give a BP-β2 variant or with the environmentally sensitive fluorophore dimethylaminonaphthalene (DAN) to give a DAN-β2 variant (Figure 1). Analysis of cross-linking between α2 and BP-β2 by SDS PAGE for all variants is reported, as are the fluorescent changes accompanying binding of DAN-β2 to α2. The results suggest that this method will be informative in acquiring molecular details and quantitative data about subunit interactions and the effects of substrates and/or effectors on these interactions.

## Materials and methods

### Materials

Benzophenone-4-maleimide (BPM) and 6-bromoacetyl-2-dimethylamino naphthalene (BADAN) were purchased from Molecular Probes (Eugene, OR). BL21 Gold (DE-3) competent cells were purchased from Stratagene (La Jolla, CA). Isopropyl-1-thio-β-D-galactopyranoside (IPTG) and 1,4-dithiothreitol (DTT) were purchased from Promega (Madison, WI). $Ni^{2+}$-NTA resin was purchased from Qiagen (Valencia, CA). 1,10-Phenanthroline, 5,5′-dithio-bis(2-nitrobenzoic acid) (DTNB), N-hydroxyurea (HU), adenosine-5′-triphosphate (ATP), cytidine-5′-diphosphate (CDP), reduced β-nicotinamide adenine dinucleotide phosphate (NADPH), kanamycin (kan) and phenylmethylsulphonyl fluoride (PMSF) were purchased from Sigma (St. Louis, MO). DNAse I and alkaline phosphatase were purchased from Roche Diagnostics (Indianapolis, IN). [5-$^3$H] Cytidine 5′-diphosphate, $NH_4$ salt (24.0 Ci/mmol) was obtained from GE Healthcare. The concentration of α2 was determined using $\varepsilon_{280}$ = 189, 000 $M^{-1}cm^{-1}$. α2 had a specific activity of 2500 nmol $min^{-1}$ $mg^{-1}$. *E. coli* thioredoxin (TR) was isolated from the overproducing strain SK3981 and had a specific activity of 40 U/mg and thioredoxin reductase (TRR) had a specific activity of 1800 U/mg (22,23).

### Methods

**Construction of β2 mutants—**Site-directed mutagenesis was carried out using a QuickChange® kit from Stratagene according to the manufacturer's protocol. pET15b-β2 which encodes $(His)_6$—β2(C268S/C305S) was used as a template for site-directed mutagenesis (24). Forward and reverse primers for the fifteen mutants are listed in supporting information (SI, Table 1). Each β2 mutant was confirmed by DNA sequencing at the MIT biopolymer facility. All mutants are $(His)_6$-β2-C268S/C305S with a single additional mutation: S341C, N343C, Q345C, A347C, Q349C, V351C, V353C, Y356C, V358C, I361C, V365C, T367C, L370C, F373C and L375C.

**Expression and purification of β2 mutants—**A plasmid encoding each β2 mutant was transformed into competent BL21 Gold (DE-3) cells. The cells were grown on LB plates (50 μg/mL kan) and incubated at 37°C overnight (~15 h). A flask containing 100 mL of LB (50 μg/mL kan) was inoculated with a single colony, and incubated on a shaker at 37°C overnight (~15 h). This subculture was then used to inoculate 2×2L at a dilution of 1:200, and incubated with shaking (200 rpm) at 37°C. At an $OD_{600}$ of ~0.7, a solution of 1,10-phenanthroline (prepared in 0.1 M HCl) was added to a final concentration of 0.1 mM (25). After 15 min, IPTG was added to a final concentration of 0.5 mM. The cells were grown for an additional 4 h and then harvested by centrifugation at 7000×g for 20 min. A typical yield was 2.5 g per L of cell culture. An SDS-PAGE gel of the cell lysate before and after induction was run to confirm successful expression.

A typical purification involved suspension of the cell pellet in 5 mL of lysis buffer (50 mM Tris, 500 mM NaCl, 10 mM imidazole, pH 7.6) per g of cells. PMSF stock was added to a final concentration of 200 μM. The cell suspension was homogenized and the cells were lysed by a single passage with the French Press at 14,000 psi. DNAse I 10 U/μL per mL (Roche) of lysate was added, and the suspension was stirred for 10 min at 4°C. The cell debris was removed by centrifugation (60000×g, 30 min). The supernatant was equilibrated with $Ni^{2+}$-NTA resin (3 mL of resin per g of cells) by gentle stirring in a beaker for 1 h at 4°C. The slurry was then loaded into a column and washed with 30 column volumes of lysis buffer. The bound protein was eluted with 200 mM imidazole in lysis buffer. The imidazole was removed by Sephadex G-25 column (2.5 × 25 cm, 20 mL) in 50 mM Tris, 5% glycerol, pH 7.6, and the protein fractions

were pooled and concentrated to ~100 μM. The yield was typically 12.5 mg of apo β2/g of cell paste.

**Reconstitution of the diferric Y• cofactor—**The reconstitution, and the determination of Y• content of each holo β2 mutant spectrophotometrically using the dropline correction method was carried out as previously described (26).

**Isolation and prereduction of α2—**The purification and prereduction of α2 were carried out as previously described (27). α2 was concentrated to 50 μM in the absence of DTT and stored in small aliquots at -80°C.

**Radioactive assay of BP-β2 variants—**A typical assay was carried out in a final volume of 200 μL which contained: 50 mM HEPES (pH 7.6), 15 mM $MgSO_4$, 1 mM EDTA, 0.1 μM BP-β2, 1.5 μM α2, 1 mM [$^3$H]-CDP (1093 cpm/nmol), 3 mM ATP, 1.0 mM NADPH, 30 μM TR, 0.5 μM TRR. All the components except BP-β2 and the [$^3$H]-CDP were mixed together. The [$^3$H]-CDP was then added and a 30 μL aliquot was removed for the zero time point. The reaction was initiated by the addition of BP-β2, and aliquots (30 μL) were removed over 4 min. All aliquots were quenched by the addition of 25 μL of 2% perchloric acid and neutralized by addition of 18 μL of 0.5 M KOH. The production of dCDP was analyzed using the method of Steeper and Steuart (28). One unit of RNR activity is defined as 1 nmol of dCDP production/min/mg.

**Determination of thiol content of β2 mutants using DTNB—**All buffers used were degassed in vacuo for at least 30 min and flushed with argon for 10 min immediately prior to use. In a typical measurement, DTT was added to β2 mutants (700 μL, 100 μM) to a final concentration of 10 mM and the solution was incubated for 30 min at 4° C. The protein was then passed through a Sephadex G-25 column (1 cm × 10 cm, 7 mL) equilibrated in degassed buffer A (50 mM HEPES, 1 mM EDTA, pH 8.0). The background spectrum of 25 μM DTNB in buffer A was recorded ($A_{410}$ denoted as A1). The protein was then diluted to 10 μM in this buffer and the background spectrum was taken ($A_{410}$ denoted as A2). DTNB was added into the cuvette containing the protein to a final concentration of 25 μM, and the UV/Vis spectrum recorded until the reaction was complete ($A_{410}$ denoted as A3). The concentration of 2-nitro-5-benzoate (TNB) and the β2 mutant in $mM^{-1}$ are given as follows: [TNB]=(A3-A2-A1)/13.6 $mM^{-1}cm^{-1}$ and [β2]=$A_{280}$/131 $mM^{-1}cm^{-1}$. The number of thiols/β2 is given by [TNB]/[β2].

**Labeling of β2 mutants with BPM—**BPM (2.5 equivalent from a 0.1 M stock solution in DMSO) was added to prereduced β2 (typically 500 μL, 75 μM) and was gently stirred at 4°C for 30 min. The solution was then centrifuged to remove undissolved BPM and passed through a Sephadex G-25 column (2 cm × 25 cm, 40 mL) equilibrated in β2 buffer (50 mM Tris, 5% glycerol, pH 7.6). The DTNB assay was performed immediately after the Sephadex G-25 column (2 cm × 25 cm, 50 mL) to determine the extent of labeling. All BP-β2 variants were characterized before and after labeling by ESI-MS.

**Labeling of β2 mutants with BADAN—**BADAN (2.5 equivalent from a 0.05 M solution in DMF) was added slowly to 150 μL of 45 μM prereduced β2 mutant with stirring at 4°C. The solution was covered with foil to protect the reaction from light and stirred for 5 h. The BADAN was removed by centrifugation and Sephadex G25 column (2 cm × 25 cm, 40 mL) equilibrated in β2 buffer. A DTNB assay could not be used to determine the extent of labeling with BADAN as it has significant absorption at 410 nm ($\lambda_{max}$ 390 nm). The concentration of DAN and β2 was determined using the following extinction coefficients: for β2, $\varepsilon_{280}$ and $\varepsilon_{390}$ are 131 $mM^{-1}cm^{-1}$ and 12.2 $mM^{-1}cm^{-1}$, respectively and for BADAN in $H_2O$ (pH 7.6), $\varepsilon_{280}$ and $\varepsilon_{390}$ are 19.8 $mM^{-1}cm^{-1}$ and 21 $mM^{-1}cm^{-1}$, respectively (Molecular Probes, Invitrogen). The

calculation to determine stoichiometry of labeling is given by [DAN]/β2, which assumes that DAN attached to β2 has the same $\varepsilon_{280}$ and $\varepsilon_{390}$ as BADAN in solution.

**ESI-MS characterization of labeled β2 variants—**Each sample for ESI-MS analysis was prepared immediately before analysis. β2 variant (15 μL of 50 μM) was exchanged into 0.1% trifluroacetic acid (TFA)/$H_2O$ using a C18 ziptip (Millipore). The sample was then diluted to a final concentration of ~5 μM with 50% MeCN, 50% $H_2O$ and 0.1% TFA. Typically, 4-5 pmol of the diluted sample was injected into the Sciex Triplequadrupole mass spectrometer (Model API 365) at 5 μL/min via direct infusion, and data were collected in positive mode.

**Photo cross-linking reaction between BP-β2 variants and α2—**To optimize the conditions for the photo cross-linking reaction, an equimolar mixture of BP-β2 and α2 (0.5 μM, 2.5 μM, 5 μM, 7.5 μM) were incubated in 40 μL of 50 mM HEPES (pH 7.6), 15 mM $MgSO_4$ and 1 mM EDTA in 96-well plate (Corning, NY). The plate was positioned underneath a hand-held UV lamp (UVP, CA, equipped with glass filter) with a ~1.4 cm distance between the lamp and the surface of the protein solution. The protein was irradiated with the lamp (~365 nm) for 30 min at 4°C. The protein from each solution was analyzed by 10% SDS-PAGE gel (2.5 μg of BP-β2, 5 μg of α2). The molecular weight and intensities of the cross-linked bands were calculated using Quantity One software (BioRad). The band intensities were normalized to the molecular weight of the cross-linked species (intensity I). In order to calculate the % of photo cross-linking, the same amount of BP-β2 (2.5 μg) and α2 (5 μg) were also loaded onto the gel, and the intensities of the bands were normalized to the molecular weight to give intensity II and intensity III, respectively. The % of cross-linked product formed was calculated from: Intensity I)/(Intensity II + Intensity III). The % of cross-linked product for each variant was then normalized to BP-β2(V365C) to obtain the relative extent of photo cross-linking.

**Characterization of DAN-β2 variants—**Fluorescence studies of DAN-β2 variants were carried out on a QM-4-SE fluorimeter from Photon Technology International (Montreal, Quebec) using FELIX software, and 2 nm excitation and 6 nm emission bandwidth slits. Measurements were performed at 22±1°C in an initial volume of 400 μL 50 mM HEPES, 15 mM $MgSO_4$, 1 mM EDTA, pH 7.6 in 500 μL microcuvettes. The excitation wavelength was 390 nm and the emission spectrum was obtained by scanning from 420-620 nm at a rate of 5 nm per sec. A similar scan of the buffer was subtracted from all other scans. In a typical experiment, the fluorescence spectrum of DAN-β2 variant (0.1 μM, 400 μL) was recorded. Prereduced α2 was then added to DAN-β2 to a final concentration of 5 μM (50-fold excess) and the fluorescence spectrum recorded. Assuming a $K_d$ of 0.4 μM for subunit interactions, addition of 5 μM would result in >95% complex formation. The intensity integrated over the full spectrum (420-620 nm) in the presence of α2 (5 μM) was subtracted from the intensity in its absence to give relative intensity ($I_r$) for each DAN-β2 variant. The relative intensity ($I_r$) for each complex of α2DAN-β2 was normalized to α2DAN-β2(V365C) to give a comparative measure of the fluorescence change.

**Determination of $K_d$ for subunit interactions—**The fluorescence spectrum of the DAN-β2 variant (0.1 μM) in 50 mM HEPES, 15 mM $MgSO_4$, 1 mM EDTA, pH 7.6 at 22±1°C was recorded to obtain the initial intensity ($I_0$) at the emission maximum. Prereduced α2 (40.0 μM) was then added in aliquots to this solution. Size exclusion chromatography (3) and sedimentation velocity methods on α suggest that it is predominantly a dimer at low μM concentrations. Thus at 40.0 μM, α is “completely” dimerized. After each addition, the sample was mixed, allowed to equilibrate, and then scanned to obtain the intensity (I). The scan was repeated to ensure equilibration. Typically, 15-20 min was required for equilibration. Addition of α2 was continued until a saturation point was reached, and the spectrum was recorded to

obtain the maximum intensity ($I_{max}$). To correct for the change in concentration, I - $I_0$ was multiplied by the appropriate dilution factor. The $K_d$ is given by the following:

$$K_d = \frac{[DAN-\beta 2]_f[\alpha 2]_f}{[\alpha 2DAN-\beta 2]} \quad (1)$$

where $[\alpha 2]_f$ and $[DAN\text{-}\beta 2]_f$ are the free concentration of α2 and DAN-β2, respectively. The above expression for $K_d$ assumes a 1:1 interaction between α2 and DAN-β2 (3), and can be reformulated as:

$$F = \frac{[\alpha 2]_f}{K_d + [\alpha 2]_f} \quad (2)$$

where *F* is the fraction of DAN-β2 complexed with α2 (i.e. $[\alpha 2DAN\text{-}\beta 2]/[DAN\text{-}\beta 2]_{total}$) and $[\alpha 2]_f$ is given by $[\alpha 2]_{total} - F \times [DAN-\beta 2]_{total}$. *F* is obtained from (29,30):

$$\frac{I - I_0}{I_{max} - I_0} \quad (3)$$

A non-linear least squares fit of the plot of *F vs*. $[\alpha 2]_f$ using prism (Graphpad) gives the $K_d$.

**Synthesis of peptide Ac-YLVGQIDSEVDTDDLSNFQL (1) and Ac-IDSEVDTD (2)—**The peptides **1** and **2** were made by solid phase peptide synthesis as previously described (24). Each product was characterized by HPLC and MALDI-TOF.

**Determination of binding of 1 and 2 to α2—**In a final volume of 400 μL, the reaction mixture contained 0.1 μM DAN-β2(V365C), 0.1 μM α2, 1mM CDP, 1 mM ATP, 50 mM HEPES, 15 mM $MgSO_4$, 1 mM EDTA, pH 7.6 at 22±1°C. The amount of α2 was calculated using a $K_d$ of 0.06 μM determined by a fluorescence titration of α2 with DAN-β2(V365C) in the presence of ATP and CDP (Hassan and Stubbe, unpublished results). The fluorescence spectrum of the above solution was recorded. Titration with **1** (2 μM to 1.0 mM) was carried out as described in the preceding section, and fluorescence intensity (I) was recorded until no further changes were observed. The intensity (I) was plotted against log [peptide] and the $IC_{50}$, the concentration of peptide required to obtain the half-maximal point of the titration, was determined using prism (Graphpad). This $IC_{50}$, was then used to calculate the $K_i$ from the following equation (31):

$$K_i = \frac{IC_{50}}{1 + \frac{[DAN-\beta 2(V365C)]_{total}(y_0+2)}{2K_d(y_0+1)} + y_0} + K_d\frac{y_0}{y_0+2} \quad (4)$$

where $K_d$ is 0.06 μM and $y_0$ is the ratio of $[DAN\text{-}\beta 2(V365C)]_{bound}$ to $[DAN\text{-}\beta 2(V365C)]_{free}$ in the absence of the peptide. Eq 4 is a modified form of the Cheng-Prusoff equation (32). Use of this equation (31) requires that the peptide is a competitive inhibitor of β2 binding to α2 and that there are two peptide binding sites on α2, one per α, that are independent of each other (18).

# Result

## Site-specific attachment of photo cross-linker and fluorescent probes to study subunit interactions

Small molecule probes have been shown to provide important tools to study protein-protein interactions (33). The two probes chosen to study the interactions between α2 and β2 are the photo cross-linker, BP (34), and the environmentally sensitive fluorescence probe, DAN (35). BP can potentially allow covalent attachment of the BP-modified residue in β2 to one or more residues in α2 in the α2β2 complex. The DAN probe in the appropriate position, on the other hand, has the potential to allow quantitation of the subunit interactions.

Theoretically, these probes could be incorporated into either α2 or β2. However, α2 contains 11 cysteines, 5 of which are essential for catalysis. Thus, generation of α2 with a single reactive cysteine, the method chosen for probe attachment, would be challenging. These challenges and the previously demonstrated importance of residues 356-375 of β2 for interaction with α2 (18,21) thus suggested that attachment of probes within this sequence would provide the best choice to study subunit interactions. An examination of the structure of β2 reveals that it has 5 Cys residues and that C268 and C305 are surface exposed (11,12). These cysteines are remote from the proposed α2β2 interface, and consequently, attachment of probes to these sites are unlikely to be good reporters of subunit interactions (8). We have previously shown that the double Cys to Ser mutation (C268S/C305S) had no effect on the enzymatic activity of *E. coli* RNR (36) and this double mutant was chosen as the starting point for all further constructs. Using β2-C268S/C305S, a single surface exposed Cys has been incorporated site-specifically into β2 through mutagenesis. Given the requirement of the C-terminal tail of β2 for interaction with α2, probe placement within this region is likely to report on this interaction. Moreover, because the C-terminal tail of β2 is unstructured and flexible (37,38), Cys introduced in this region will likely be accessible for labeling with thiol reactive probes. Our strategy is summarized in Figure 1.

## Selection of the residues for probe attachment

The crystal structure of α2 in complex with the 20 residue C-terminal peptide of β2 (356-375) guided the selection of residues for probe attachment (8,13). Eighteen residues (358-375) of the peptide are visible. The structure shows that majority of the peptide adopts a reverse turn configuration and is sandwiched between helix αI and α13. The side chains of residues V358, I361, V365, T367, L370, F373 and L375 of the peptide are projected towards α2. Each of these residues was, therefore, mutated to a Cys and then labeled with BP and DAN. Because no information is available about residues 341-357, Cys mutations were arbitrarily placed at every other position within this region. These fifteen residues were selected for probe attachment.

## Generation and characterization of β2 mutants

The Cys mutations were introduced by site-directed mutagenesis using N-terminal $(His)_6$ tagged *nrdB* (N terminal GHHHHHHM-β2) with C268S/C305S mutations as the template (SI, Table 1). The $(His)_6$ tag facilitated the rapid purification of the mutants and does not have any significant effect on the enzymatic activity (24). The growth of *E. coli* and expression of the mutants were carried out in the presence of the iron-chelator 1,10-phenanthroline resulting in purification of all fifteen mutants in the apo form (25). The diferric Y• cofactor was then reconstituted *in vitro* by standard procedures (26). The yield and the radical content of reconstituted holo mutants suggest that these cysteine mutations had little effect on the expression level of the protein or the assembly of the active cofactor (SI, Table 2). Assay with Ellman's reagent (DTNB) showed that each mutant had 1.9-2.1 surface accessible thiols/β2. Activity assays with the Cys mutants showed that the mutation in general reduced activity from 6000 μmol/min/mg (observed for the wt-β2) to 11 - 2586 nmol/min/mg (0.2 to 43 % of the wt-

β2 activity) depending on the location within the tail (Table 2). In the following sections, a specific β2 mutant such as $(His)_6$—β2-C268S/C305S/V365C is denoted as β2(V365C).

## Labeling of β2 mutants with BP and DAN

BPM was chosen to attach the BP probe to β2 (Figure 1). The reaction conditions for the Michael addition between the thiolate of the mutant β2 and BPM were optimized by monitoring the reaction using the DTNB assay. A typical protocol involved incubation of 75 μM mutant β2 with 187 μM BPM at 4°C for 30 min at which time the reaction was complete. Each BP-β2 was purified and characterized by ESI-MS. In each case, the presence of a peak with the expected mass (within the error of the method <20 ppm) for BP-β2 and the absence of a peak for unlabeled β2 supported stoichiometric labeling (SI, Table 3). Each mass spectrum also showed a second species with a mass of 170-180 Da greater than the expected mass of the BP-β2 variants (SI, Figure 1). This second species has been observed previously in the mass spectra of wt-β2, $(His)_6$-β2 and semi-synthetic β2 (24). The basis for this increase in mass is not understood. In addition, each mutant was characterized for its ability to make deoxynucleotides using an assay with [$^{14}$C]-CDP (Table 2). BP-modification in general reduced activity to 3 - 1100 nmol/min/mg (0.07 to 8.1 % of the wt-β2 activity) depending on the location within the tail. The lower limit of activity detection was 0.6 nmol/min/mg, thus all mutants are active.

The labeling of the Cys mutants with DAN was accomplished by $S_N2$ displacement of bromide from BADAN by the Cys thiolate. Optimized reaction conditions employed 75 μM β2 mutant with 2.5 equivalent of BADAN at 4°C for 5 h. Using the molar extinction coefficients of DAN and β2 at 280 and 390 nm, the stoichiometry of DAN/β2 was determined spectrophotometrically. It ranged from 1.9 to 2.2, with the variability likely due to the changes in DAN absorbance depending on its location within β2, relative to free DAN. The ESI-MS of variants 356, 361, 365 and 367 were determined and found to be identical to the expected values (SI, Table 4). As with the BP-β2 variants, additional mass of 170-180 Da was also observed with DAN-β2 variants. Activity assays of the four variants ranged from 0.1 to 13 % of the wt-β2 (Table 2).

## Photo cross-linking reaction between BP-β2 variants and α2

To maximize the photo cross-linking reaction between α2 and BP-β2 variants, the temperature, the time of exposure to light and the subunit concentrations of α2 and BP-β2 were varied. In an optimized experiment, 5 μM α2 and BP-β2 were irradiated at ~365 nm for 30 min at 4°C, and then analyzed by SDS-PAGE. The results are shown in Figure 2. The molecular weights of α and BP-β are ~87 kDa and 44 kDa, respectively and that of 1:1 complex of αBP-β is ~131 kDa. The percentage of cross-linking was calculated by comparison of the intensity of the 131 kDa band with that of α and BP-β bands in the absence of light. This analysis shows that the yield of the photo cross-linked product varies from 3% to 19%, with BP labeling at 361, 365, 367 giving the highest yields (SI, Table 5). The location of Y356 is particularly important to establish given the absence of structural information, its essential role in radical propagation between α2 and β2 and the proposed distance of 25Å between W48 in β2 and Y731 in α2 based on the docking model (8). The BP-β2(Y356C) variant shows ~9% cross-linking. BP variants in the region of 341-357 and at positions 373 and 375 near the C-terminus show 3-5% cross-linking. Efforts to increase the cross-linking efficiency by addition of substrate and/or effector to α2 and BP-β2 in which the Y• was reduced were unsuccessful. Finally, in addition to the photo cross-linked product observed at 131 kDa, a band of varying intensity with a molecular weight ~250 kDa was also present in BP modified residues 347-365. The molecular weight analysis suggests that this band may be a complex of α2BP-β2 (~260 kDa). A possible mechanism for its formation will be discussed subsequently.

### Fluorescence characterization of DAN-β2 variants with α2

The fluorescence spectrum of each DAN-β2 variant was acquired in the presence of saturating amounts of α2, where the emission maxima μranged from 496-522 nm. The fluorescence spectra of a number of α2DAN-β2 variant complexes are shown in Figure 3. A comparison of the results shows differences in emission intensity, maxima, or both depending on the location of the probe (SI, Table 6). DAN-β2 (Y356, I361C, V365C and T367C) show significant increases in fluorescence intensity with minimal change in emission maxima. DAN-β2 (F375C), in contrast, shows both an increase in fluorescence intensity and a shift in emission maximum. Finally, DAN-β2(N343C and L345C) show very little change in fluorescence intensity or emission maximum.

### Position dependent comparison of the extent of photo cross-linking and change in fluorescence of the β2 variants

The percentage of photo cross-linking and the change in fluorescence intensity of each BP-β2 and DAN-β2 variant were normalized to the values observed for β2(V365C), the variant with the largest changes in both cases (Figure 4). The extent of photo cross-linking parallels the changes in fluorescence intensity, with the largest changes being observed in residues 361, 365, 367. These studies suggest that 361-367 of the C-terminal tail of β2 might play an important role in subunit interactions. As discussed subsequently, competitive binding studies with peptides composed of these residues were carried out in an attempt to better understand the role of this region in subunit interactions.

### Determination of $K_d$ for subunit interactions with DAN-β2 variants

The large increase in fluorescence intensity of DAN-β2(V365C) upon addition of α2 made this variant a good candidate to probe the binding affinity of α2 and β2, and thus DAN-β2(V365C) was titrated with increasing concentrations of α2 at 22°C in the absence of allosteric effectors or substrates. As noted above, α in the absence of nucleotides is a mixture of dimers and monomers (3). Our titration experiments assume that α2 binds to β2 generating additional α2. The $K_d$ for α2 has not been determined. However our preliminary results suggest that α is predominantly dimer (α2) under the titration conditions.

The results of a typical titration are shown in Figure 5. Analysis of these data gave a $K_d$ of 0.36 ±0.07 μM (Figure 6). The assumption has been made that at the end of the titration the predominant species is a 1:1 complex of α2 and β2. Modification of a residue involved in subunit interactions is likely to alter the measurement of interest. This alteration in case of residue 365 is apparent from the reduced activity in nucleotide reduction (10% wt activity). Thus, similar measurements were made with DAN attached to 351, 356 and 367. Residue 367 was chosen because of its similar behavior to 365 in the presence of α2 including its activity (Table 2). Residue 356 was chosen due to its importance in radical propagation between the subunits and the likely possibility that its position moves during binding and catalysis. Finally, residue 351 was chosen, as the previous studies with peptides to C-terminal tail of β2 suggested that residues 340 to 355 have a small effect on subunit interactions (18,21). Neither 356, nor 351 is observed in any crystal structure. Despite the different behaviors of these DAN-β2 variants, the titration studies surprisingly gave similar $K_d$s (Table 1). No previous studies have reported a quantitative assessment of α2β2 interactions in the absence of nucleotides.

### Determination of $K_d$s for 1 and 2 with α2

The observed fluorescence changes upon α2DAN-β2 complex formation suggest a screen for inhibitors of subunit interactions and a way to assess the importance of residues 361-367 of β2 in this interaction. As proof of concept, we examined a peptide composed of residues Y356 to L375 of β2 with the N-terminus acetylated. This peptide was previously shown to inhibit

subunit interaction with a $K_i$ (equivalent to $K_d$) of 20 μM (18). The loss of fluorescence from the α2DAN-β2(V365) complex upon titration with increasing concentration of peptide should allow determination of its $K_d$.

In designing a fluorescence-based competitive assay, two factors are important (29,30): the ratio between probe (DAN-β2) and receptor (α2), and the dynamic range of the assay i.e. the change in the signal (fluorescence intensity or polarization) between free and bound probe. Since the optimized concentration of DAN-β2(V365C) used in the $K_d$ determination gives rise to a large change in fluorescence intensity (Figure 5), both DAN-β2(V365C) and α2 at 0.1 μM were chosen to carry out a competitive titration study. Finally titrations were carried out in the presence of nucleotide to potentiate α dimerization. Increasing amounts of peptide **1** were added to α2DAN-β2(V365C) resulting in loss of fluorescence intensity at the emission maxima, ~503 nm. A plot of relative intensity *vs*. Log [peptide] allowed determination of the $IC_{50}$ (Figure 7), which was then used to calculate $K_i$ (equivalent to $K_d$) of 16.6 ± 2.7 μM (Eq 4). The $K_d$ for peptide 1 is ~40 fold higher than for DAN-β2 variants. A difference of ~100 fold was found between the interaction of wt-β2 with α2 ($K_i = K_d = 0.2$ μM) and with the C-terminal peptide of β2 (residues 353 to 375, $K_d = K_i = 20$ μM) (18). Insight into the basis for the differences in $K_d$s between full length β and the peptides was obtained from two independent studies where heterodimer of β2, ββ', (where β is full length protein with residues 1-375 and β' is missing the last 22 amino acids or 24 amino acids) have $K_d$s of 6.5 μ M (18, 21) and 11 μM (39). In addition, β'β' showed no binding (40). These studies initially allowed Sjöberg and her coworkers to invoke a chelate effect, where binding of one β2 tail to α potentiates binding to the second second tail to α (18,21).

As noted above and summarized in Figure 4, there appears to be a correlation between sites resulting in the most extensive cross-linking and those associated with largest increases in fluorescence. Having established the validity of the competitive assay with **1**, an acylated octamer, **2** (Ac-IDSEVDTD), was synthesized to test the importance of these residues in the inhibition of subunit interactions. A titration with concentrations of **2** up to 10 mM peptide resulted in no loss in fluorescence intensity. Thus, this region by itself does not appear to be responsible for the predominant interactions with α2. This result might have been predicted from studies of Climent *et al*(18) in which they determined $K_d$s for peptides corresponding to the C-terminus of β [peptide 1-8 (residues 368-375), 12-20 (residues 356-364), 1-19 (residues 357-375), 1-20 (residues 356-375) and 1-30 (residues 346-375)]. The acylated 8 mer (1-8) has a $K_d$ of ~400 μM, while the 19 mer (1-19) has a $K_d$ of 40 μM. Only a difference of 10 fold is associated with residues 9-19. Thus, lack of binding of our peptide 2 (8-15) suggests once again, the importance of the 'chelate effect' where binding of the C-terminus of β potentiates an additional small amount of binding associated with residues 8-15; without the C-terminus, thus no binding of 2 would be expected.

## Discussion

The present communication documents the site-specific incorporation of the photo cross-linker (BP) and the environmentally sensitive probe (DAN) into intact β2 of RNR to probe subunit interactions. The studies with BP-β2 variants reveal that the cross-linking occurs to some extent at each site of BP attachment (Figure 2), with the highest extent of cross-linking occurring between 356 and 370. Photo cross-linking efficiency for the catalytically important Y356 is observed, however, at only 9% efficiency. We have recently synthesized the [$^{14}$C]-iodoacetamide analog of benzophenone ([$^{14}$C]-BPI), and analyzed the cross-linking sites with β2(V365C) variant using trypsin digestion and Edman sequencing (41). Cross-links to 356 (either to α2 or within β2) are of particular interest as they might report on the flexibility of this residue during catalysis. The possibility of multiple interactions and the low level of cross-linking, however, will make this analysis challenging. An additional interesting observation

from the cross-linking experiments is the presence of a higher molecular weight species (~250 kDa) with BP-modified residues between 349 to 365. The nature of the complex is unknown, but the size suggests that the complex is composed of 2αs and 2βs. A control photo cross-linking experiment of BP-β2(V365C) in the absence of α2 was carried out. SDS PAGE analysis showed the presence of only monomeric β, excluding the formation of an inter-subunit cross-linking. To obtain a species with >250 kDa, one would need to assume that the cross-linking between α and β enhances the interaction for free α and β such that the complex is stable under SDS-PAGE conditions. Such a large molecular weight aggregate has recently been observed when gemcitabine diphosphate inactivates RNR (3). Further experiments are required to test the validity of the model.

DAN labeled β2s were of interest for two reasons. First, the $K_d$s for the interactions between α2 and β2 in the presence of NDP substrates and/or dNTP effectors pairs have not been determined systematically (18,20,21). A quantitative model for allosteric regulation of RNRs must include an understanding of subunit interactions and the changes in the interactions in the presence of nucleotides. Second, fluorescence methods are now widely used in high through put screening (29,30) to monitor inhibition of protein-protein interactions. Thus, DAN-β2 variants could also serve as a tool to find new antibacterial agents.

The DAN fluorophore was chosen as a probe because of its small size, high extinction coefficient and environmentally sensitive properties (35,42). In $H_2O$, DAN has an emission maximum of ~550 nm, which blue shifts and shows increases in intensity in a non-polar environment. The docking model of α2β2 has, in part, been guided by the co-crystallization of α2 with a peptide corresponding to residues 356-375 of β2. The changes in fluorescence intensities and emission maxima are consistent with the hydrophobic environment that residues 361, 365, 367, 370, 373 and 375 encounter on binding based on the model (SI, Table 7).

To demonstrate the usefulness of the DAN-β2 variants for the determination of the $K_d$ for subunit interactions, and to assess the perturbation that might be affiliated with the probe, four different variants were chosen for fluorescence titration studies. Surprisingly, the measured $K_d$s for all four variants examined were almost identical (0.34 to 0.41 μM). These numbers are two fold higher than the $K_d$s previously reported based on a kinetic analysis to determine $K_i$s for peptide inhibition (18,21). However, in these experiments, the presence of CDP and ATP might account for the differences. Our studies suggest that DAN-β2 variants will be useful to quantitate the relative changes in subunit interactions in the presence of nucleotides. A quantitative and comprehensive analysis of the subunit interactions is key component to a better understanding of allosteric regulation of RNRs and will be the subject of future reports.

The differences in the sequences of the C-termini of β2 from bacteria, viruses and humans, the importance of subunit interaction in all cases for the formation of active RNR and the essentiality of RNR for cell survival suggest that subunit disruption could be a therapeutically important target (17,43). Studies with peptidomimetics of the C-terminal tail of herpes simplex virus (HSV) RNR have been investigated as potential anti HSV agents (17,43), and peptides to C-terminal tail of β2 from mouse RNR have been explored as potential anti-cancer agents (17,44). A high through-put screen of small molecule libraries could facilitate identification of lead compounds to inhibit α2β2 interactions and thus RNR activity. Our preliminary data using a competitive fluorescence titration with **1** gave a $K_d$ of 16.6 ± 2.7 μM, similar to the value previously determined by an independent method (18). Thus, monitoring fluorescence losses could provide a rapid high through-put screening method for finding lead inhibitors.

## Summary

The methodology described in this manuscript offers new probes to determine the molecular basis for interactions between the subunits of RNR and to measure their affinities in the

presence of different substrate and/or effector pairs. These methods can be readily extended to RNRs from other sources and should be generally useful for unraveling the complexities of these flexible proteins.

## Supplementary Material

Refer to Web version on PubMed Central for supplementary material.

## Abbreviation

RNR, ribonucleotide reductase
α2, ribonucleotide reductase large subunit
β2, ribonucleotide reductase small subunit
NDP, nucleoside diphosphate
NTP, nucleoside triphosphate
ATP, adenosine-5′-triphosphate
CDP, cytidine-5′-diphosphate
dNDP, deoxynucleoside-5′-diphosphate
dNTP, deoxynucleoside-5′-triphosphate
NADPH, reduced β-nicotinamide adenine dinucleotide phosphate
BPM, benzophenone-4-maleimide
BADAN, 6-bromoacetyl-2-dimethylaminonaphthalene
DAN, dimethylaminonaphthalene
BP, benzophenone
DAN-β2, DAN labeled β2
BP-β2, BP labeled β2
DAN-β2(V365C), DAN labeled β2 at V365C
BP-β2(V365C), BP labeled β2 at V365C
HU, N-hydroxyurea
Y•, tyrosyl radical
TR, thioredoxin
TRR, thioredoxin reductase
DTNB, dithio-bis(2-nitrobenzoic) acid
Kan, Kanamycin
PMSF, phenylmethylsulphonyl fluoride
TNB, 2-nitro-5-thiobenzoate.

## Reference

(1). Stubbe J, van der Donk WA. Protein radicals in enzyme catalysis. Chem. Rev 1998;98:705–762. [PubMed: 11848913]

(2). Jordan A, Reichard P. Ribonucleotide reductases. Annu. Rev. Biochem 1998;67:71–98. [PubMed: 9759483]

(3). Wang J, Lohman GJS, Stubbe J. Enhanced subunit interactions with gemcitabine-5 ′-diphosphate inhibit ribonucleotide reductases. Proc. Natl. Acad. Sci. U.S.A 2007;104:14324–14329. [PubMed: 17726094]

(4). Brown NC, Reichard P. Ribonucleoside diphosphate reductase : Formation of active and inactive complexes of proteins B1 and B2. J. Mol. Biol 1969;46:25–38. [PubMed: 4902211]

(5). Thelander L. Physicochemical characterization of ribonucleoside diphosphate reductase from *Escherichia coli*. J. Biol. Chem 1973;248:4591–4601. [PubMed: 4578086]

(6). Sjöberg BM, Reichard P, Gräslund A, Ehrenberg A. Nature of free-radical in ribonucleotide reductase from *Escherichia coli*. J. Biol. Chem 1977;252:536–541. [PubMed: 188819]

(7). Sjöberg BM, Reichard P, Gräslund A, Ehrenberg A. Tyrosine free-radical in ribonucleotide reductase from *Escherichia coli*. J. Biol. Chem 1978;253:6863–6865. [PubMed: 211133]

(8). Uhlin U, Eklund H. Structure of ribonucleotide reductase protein R1. Nature 1994;370:533–9. [PubMed: 8052308]

(9). Uppsten M, Farnegardh M, Domkin V, Uhlin U. The first holocomplex structure of ribonucleotide reductase gives new insight into its mechanism of action. J. Mol. Biol 2006;359:365–77. [PubMed: 16631785]

(10). Eklund H, Uhlin U, Farnegardh M, Logan DT, Nordlund P. Structure and function of the radical enzyme ribonucleotide reductase. Prog. Biophys. Mol. Biol 2001;77:177–268. [PubMed: 11796141]

(11). Nordlund P, Eklund H. Structure and function of the *Escherichia coli* ribonucleotide reductase protein R2. J. Mol. Biol 1993;232:123–164. [PubMed: 8331655]

(12). Nordlund P, Sjöberg BM, Eklund H. Three-dimensional structure of the free radical protein of ribonucleotide reductase. Nature 1990;345:593–8. [PubMed: 2190093]

(13). Eriksson M, Uhlin U, Ramaswamy S, Ekberg M, Regnstrom K, Sjöberg BM, Eklund H. Binding of allosteric effectors to ribonucleotide reductase protein R1: reduction of active-site cysteines promotes substrate binding. Structure 1997;5:1077–1092. [PubMed: 9309223]

(14). Bennati M, Robblee JH, Mugnaini V, Stubbe J, Freed JH, Borbat P. EPR distance measurements support a model for long-range radical initiation in *Escherichia coli* ribonucleotide reductase. J. Am. Chem. Soc 2005;127:15014–15015. [PubMed: 16248626]

(15). Seyedsayamdost MR, Chan CTY, Mugnaini V, Stubbe J, Bennati M. PELDOR spectroscopy with DOPA-β2 and NH2Y-α2s: Distance measurements between residues involved in the radical propagation pathway of *Escherichia coli* ribonucleotide reductase. J. Am. Chem. Soc 2007;129:15748–15749. [PubMed: 18047343]

(16). Cohen EA, Gaudreau P, Brazeau P, Langelier Y. Specific-inhibition of herpesvirus ribonucleotide reductase by a nonapeptide derived from the carboxy terminus of subunit-2. Nature 1986;321:441–443. [PubMed: 3012360]

(17). Cooperman BS. Oligopeptide inhibition of class I ribonucleotide reductases. Biopolymers 2003;71:117–131. [PubMed: 12767114]

(18). Climent I, Sjöberg BM, Huang CY. Carboxyl-terminal peptides as probes for *Escherichia coli* ribonucleotide reductase subunit interaction - kinetic-analysis of inhibition studies. Biochemistry 1991;30:5164–5171. [PubMed: 2036382]

(19). Ingemarson R, Thelander L. A kinetic study on the influence of nucleoside triphosphate effectors on subunit interaction in mouse ribonucleotide reductase. Biochemistry 1996;35:8603–9. [PubMed: 8679622]

(20). Kasrayan A, Birgander PL, Pappalardo L, Regnstrom K, Westman M, Slaby A, Gordon E, Sjöberg BM. Enhancement by effectors and substrate nucleotides of R1-R2 interactions in *Escherichia coli* class Ia ribonucleotide reductase. J. Biol. Chem 2004;279:31050–31057. [PubMed: 15145955]

(21). Climent I, Sjöberg BM, Huang CY. Site-directed mutagenesis and deletion of the carboxyl terminus of *Escherichia coli* ribonucleotide reductase protein R2 - effects on catalytic activity and subunit interaction. Biochemistry 1992;31:4801–4807. [PubMed: 1591241]

(22). Russel M, Model P. Direct cloning of the trxB gene that encodes thioredoxin reductase. J. Bacteriol 1985;163:238–42. [PubMed: 2989245]

(23). Lunn CA, Kathju S, Wallace BJ, Kushner SR, Pigiet V. Amplification and purification of plasmid-encoded thioredoxin from *Escherichia coli* K12. J. Biol. Chem 1984;259:10469–74. [PubMed: 6381486]

(24). Yee CS, Seyedsayamdost MR, Chang MCY, Nocera DG, Stubbe J. Generation of the β2 subunit of ribonucleotide reductase by intein chemistry: Insertion of 3-nitrotyrosine at residue 356 as a probe of the radical initiation process. Biochemistry 2003;42:14541–14552. [PubMed: 14661967]

(25). Baldwin J, Krebs C, Ley BA, Edmondson DE, Huynh BH, Bollinger JMJ. Mechanism of rapid electron transfer during oxygen activation in the R2 subunit of *Escherichia coli* ribonucleotide reductase. 1. Evidence for a transient tryptophan radical. J. Am. Chem. Soc 2000;122:12195–12206.

(26). Bollinger JM, Tong WH, Ravi N, Huynh BH, Edmondson DE, Stubbe J. Use of rapid kinetics methods to study the assembly of the diferric-tyrosyl radical cofactor of *Escherichia coli*

ribonucleotide reductase. Methods Enzymol. (Redox-Active Amino Acids in Biology) 1995:278–303.

(27). Mao SS, Holler TP, Yu GX, Bollinger JM, Booker S, Johnston MI, Stubbe J. A model for the role of multiple cysteine residues involved in ribonucleotide reduction - amazing and still confusing. Biochemistry 1992;31:9733–9743. [PubMed: 1382592]

(28). Steeper JR, Steuart CD. A rapid assay for CDP reductase activity in mammalian cell extracts. Anal. Biochem 1970;34:123–130. [PubMed: 5440901]

(29). Kenny CH, Ding WD, Kelleher K, Benard S, Dushin EG, Sutherland AG, Mosyak L, Kriz R, Ellestad G. Development of a fluorescence polarization assay to screen for inhibitors of the FtsZ/ZipA interaction. Anal. Biochem 2003;323:224–233. [PubMed: 14656529]

(30). Lasagna M, Vargas V, Jameson DM, Brunet JE. Spectral properties of environmentally sensitive probes associated with horseradish peroxidase. Biochemistry 1996;35:973–979. [PubMed: 8547280]

(31). Munson PJ, Rodbard D. An exact correction to the Cheng-Prusoff correction. J. Recept. Res 1988;8:533–546. [PubMed: 3385692]

(32). Cheng Y, Prusoff WH. Relationship between inhibition constant (KI) and concentration of inhibitor which causes 50 per cent inhibition (I50) of an enzymatic-reaction. Biochem. Pharmacol 1973;22:3099–3108. [PubMed: 4202581]

(33). Imperiali B, Shults MD, Vazquez E, Rothman DM, Janes KA, Nguyen A, Lauffenburger DA, Yaffe MB. Chemical tools for the study of complex biological systems. Mol. Biol. Cell 2004;15:245A–245A. [PubMed: 14565978]

(34). Dorman G, Prestwich GD. Benzophenone photophores in biochemistry. Biochemistry 1994;33:5661–5673. [PubMed: 8180191]

(35). Farris FJ, Weber G, Chiang CC, Paul IC. Preparation, crystalline-structure, and spectral properties of fluorescent-probe 4,4-bis-1-phenylamino-8-naphthalenesulfonate. J. Am. Chem. Soc 1978;100:4469–4474.

(36). C.S., Y. PhD Thesis. MIT; Cambridge, MA: 2004.

(37). Lycksell PO, Ingemarson R, Davis R, Gräslund A, Thelander L. 1H-NMR studies of mouse ribonucleotide reductase - the R2 protein carboxyl-terminal tail, essential for subunit interaction, is highly flexible but becomes rigid in the presence of protein R1. Biochemistry 1994;33:2838–2842. [PubMed: 8130196]

(38). Lycksell PO, Sahlin M. Demonstration of segmental mobility in the functionally essential carboxyl-terminal part of ribonucleotide reductase protein R2 from *Escherichia coli*. FEBS Lett 1995;368:441–444. [PubMed: 7635194]

(39). Seyedsayamdost MR, Stubbe J. Forward and reverse electron transfer with the Y(356)DOPA-β2 heterodimer of *Escherichia coli* ribonucleotide reductase. J. Am. Chem. Soc 2007;129:2226–2227. [PubMed: 17279757]

(40). Sjöberg BM, Karlsson M, Jornvall H. Half-site reactivity of the tyrosyl radical of ribonucleotide reductase from *Escherichia coli*. J. Biol. Chem 1987;262:9736–43. [PubMed: 3298261]

(41). Hassan AQ, Stubbe J. Mapping the subunit interface of ribonucleotide reductase (RNR) using photo cross-linking. Bioorg. Med. Chem. Lett. 2008In press

(42). Weber G, Farris FJ. Synthesis and spectral properties of a hydrophobic fluorescent-probe - 6-propionyl-2-(dimethylamino)Naphthalene. Biochemistry 1979;18:3075–3078. [PubMed: 465454]

(43). Liuzzi M, Deziel R, Moss N, Beaulieu P, Bonneau AM, Bousquet C, Chafouleas JG, Garneau M, Jaramillo J, Krogsrud RL, Lagace L, McCollum RS, Nawoot S, Guindon Y. A potent peptidomimetic inhibitor of Hsv ribonucleotide reductase with antiviral activity *in-vivo*. Nature 1994;372:695–698. [PubMed: 7990963]

(44). Gao Y, Tan C, Kashlan OB, Kaur J, Cooperman BS. New peptide inhibitors of mammalian ribonucleotide reductase. Mechanisms of action. Regulatory Peptides 2004;122:14–14.

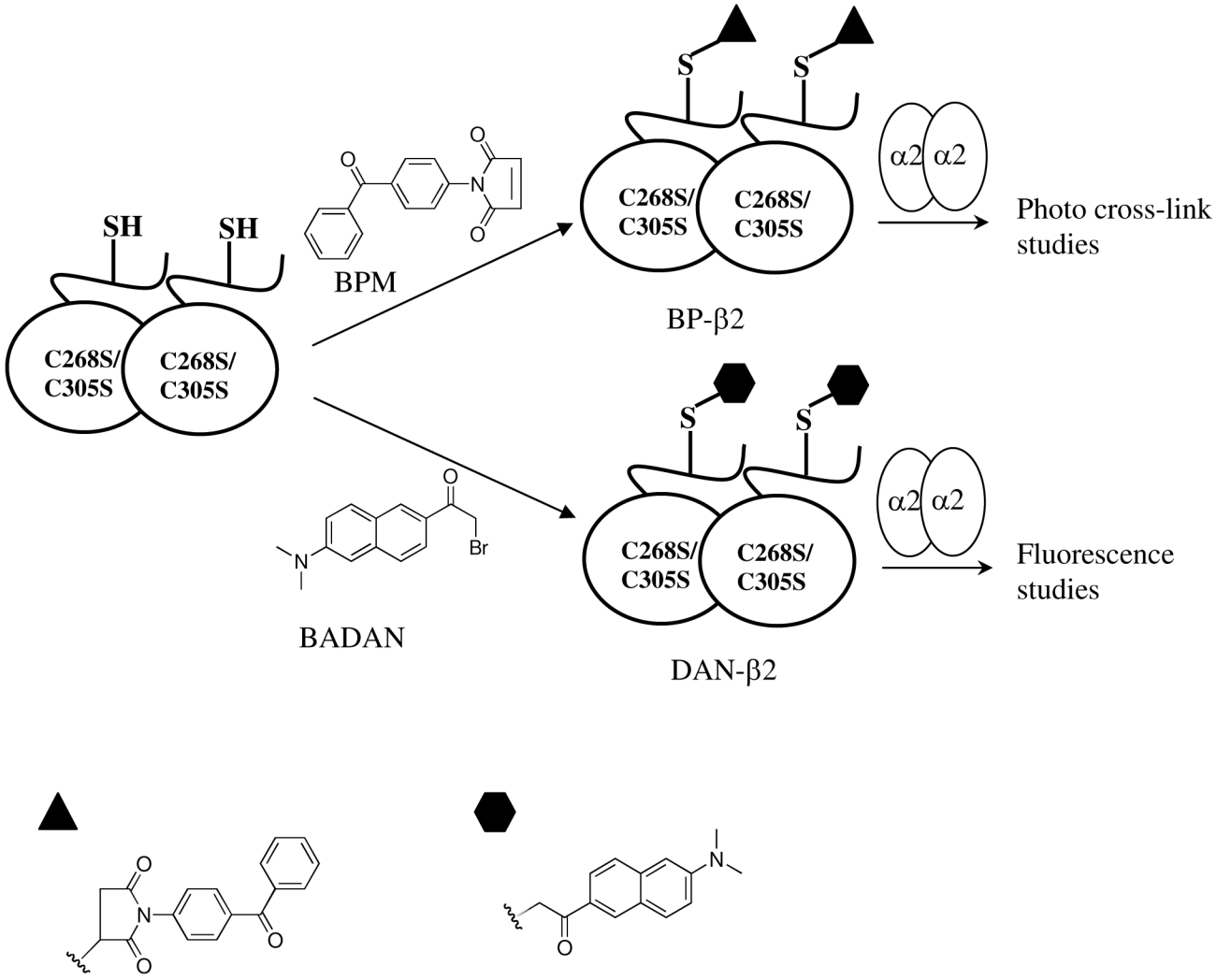


**Figure 1.**
Strategy for site-specific labeling of β2. A single Cys is placed within the C-terminal tail of β2 and then labeled with the photo cross-linker (BP) or the environmentally sensitive fluorophore (DAN).

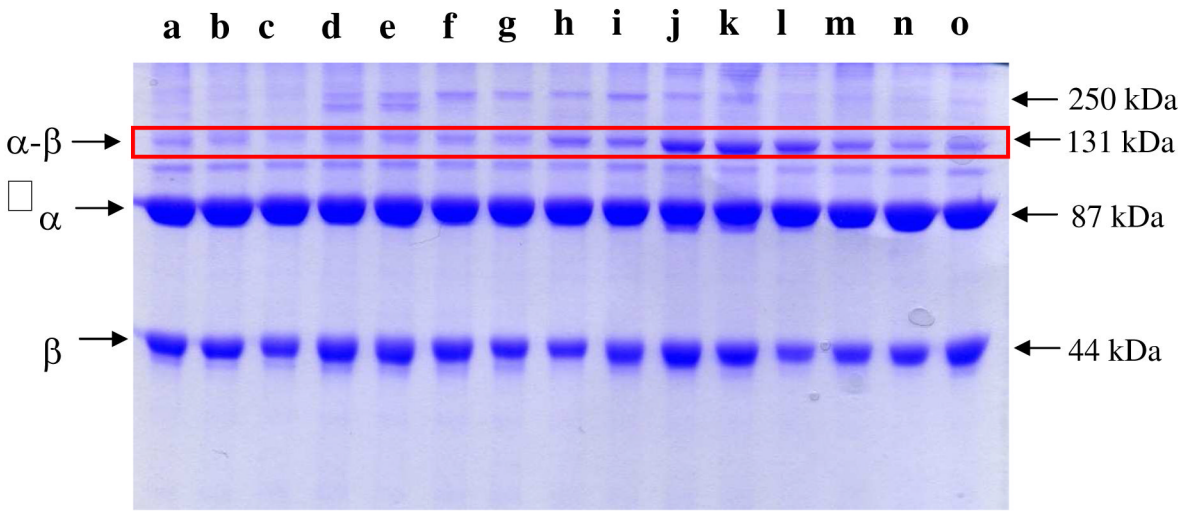


**Figure 2.**

Photo cross-linking reaction between each BP-β2 variant and α2. α (~87 kDa), BP-β variant (~44 kDa) and cross-linked product α-BP-β (131 kDa, box) are indicated with arrows. The band underneath the cross-linked product is a contaminant (~110 kDa) that co-purifies with α2. A band corresponding to ~250 kDa is also shown. Each lane represents cross-linking of a different BP-β2 variant: a. S341C; b. N343C; c. Q345C; d. A347C; e. Q349C; f. V351C; g. V353C; h. Y356C; i. V358C; j. I361C; k. V365C; l. T367C; m. L370C; n. F373C; o. L375C.

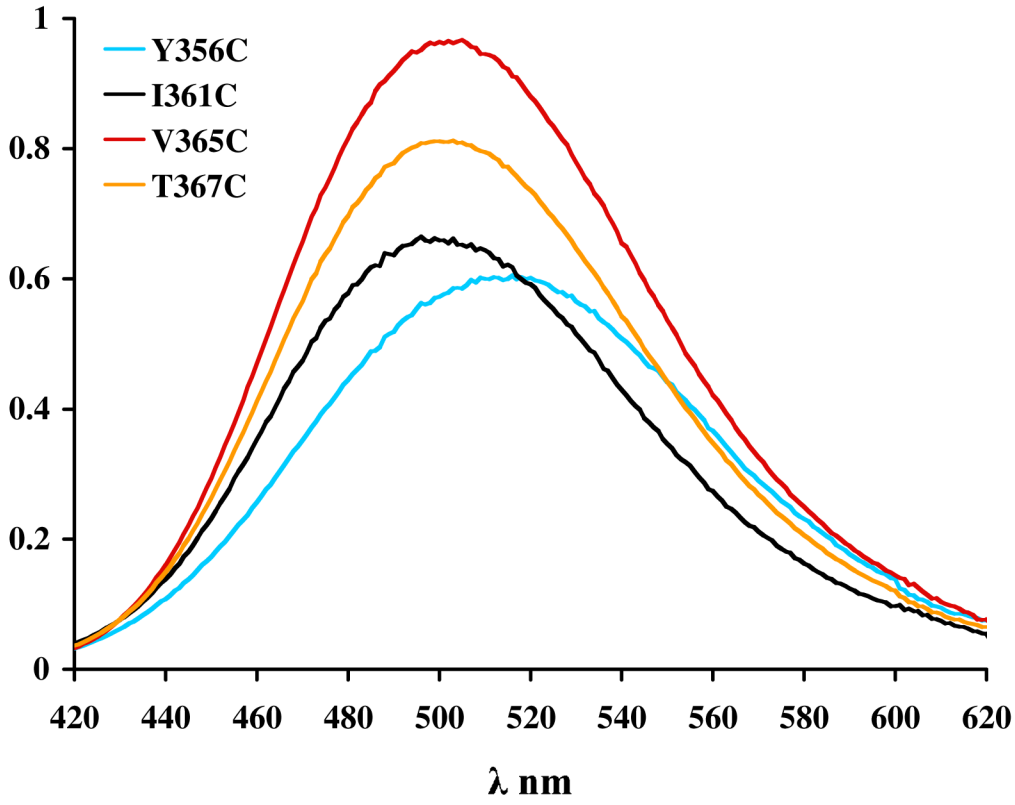


**Figure 3.**

The fluorescence spectra of four DAN-β2 variants (0.1 μM) in complex with 5 μM of α2 in 50 mM HEPES, 15 mM $MgSO_4$, 1 mM EDTA, pH 7.6 at 22°C. The excitation wavelength was 390 nm and the emission spectra were collected from 420-620 nm.

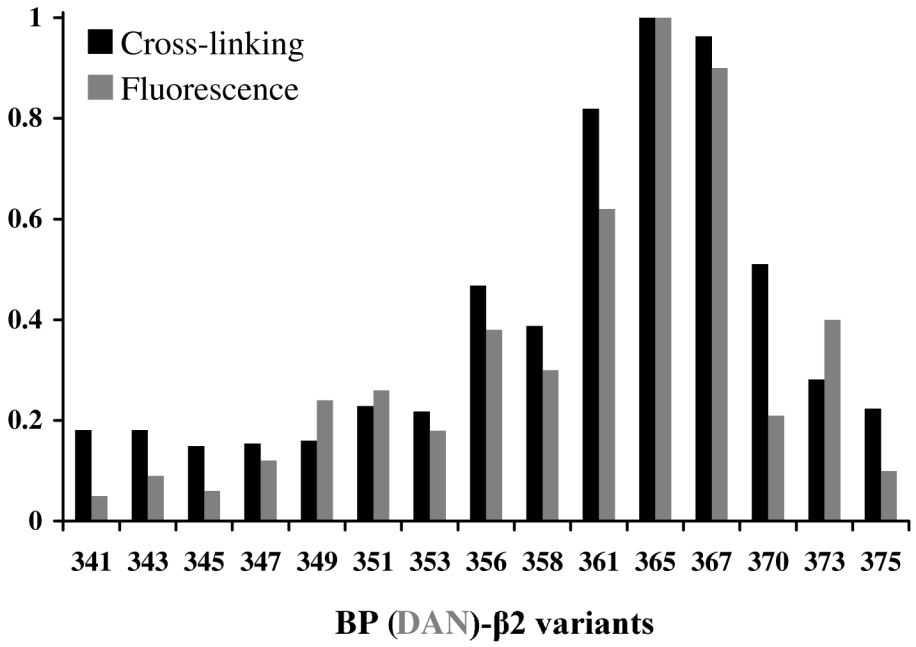


**Figure 4.**

Comparison of the relative extent of photo cross-linking reaction (■) of each BP-β2 variant relative to BP-β2 (V365C) and the increases in fluorescence intensity (■) of each DAN-β2 relative to DAN-β2 (V365C).

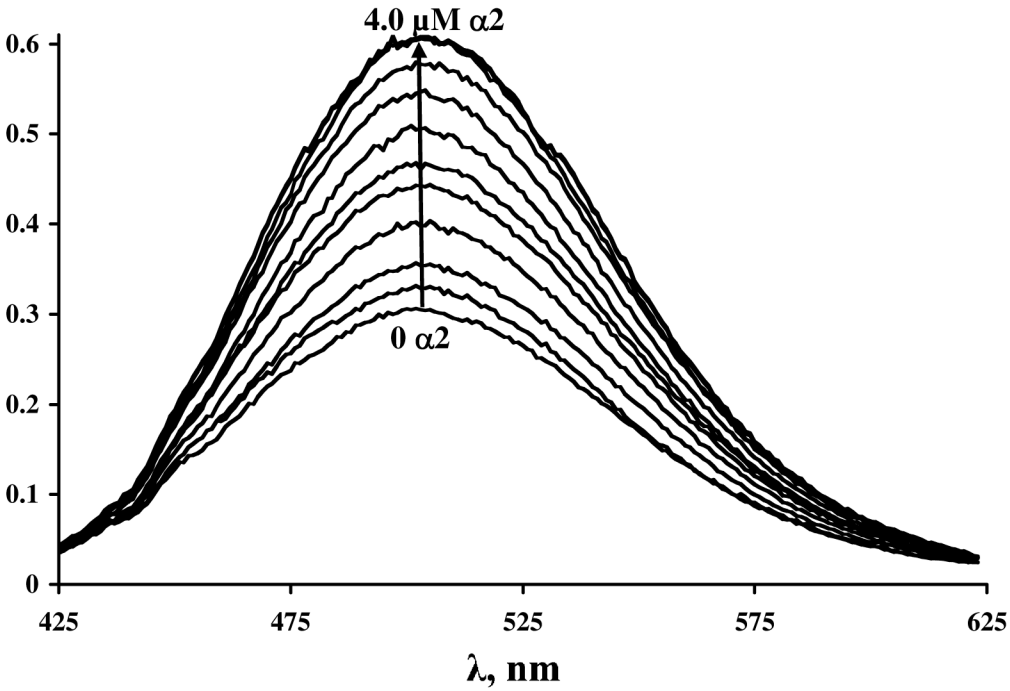


**Figure 5.**

Fluorescence titration of DAN-β2 (V365C) with increasing amounts of α2 (0 to 4.0 μM). Measurements were carried out in 50 mM HEPES, 15 mM $MgSO_4$,1 mM EDTA, pH 7.6 at 22°C.

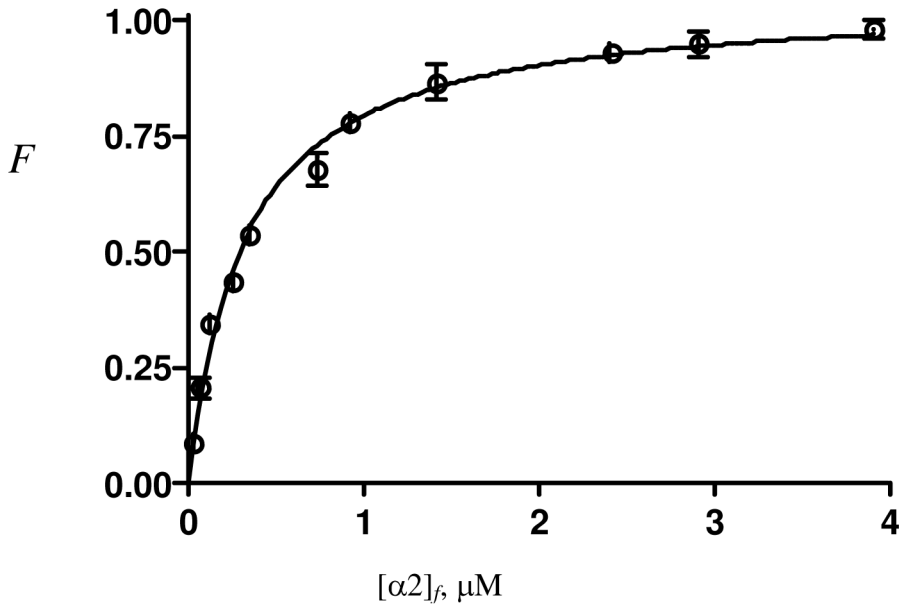


**Figure 6.**

Plot of *F vs*. $[\alpha 2]_f$ to determine the $K_d$ for α2DAN-β2 (V365C) in the absence of substrate and effector. Measurements were carried out at 22±1°C in 50 mM HEPES, 15 mM $MgSO_4$, 1 mM EDTA, pH 7.6. Error bars are the standard deviation of three independent measurements.

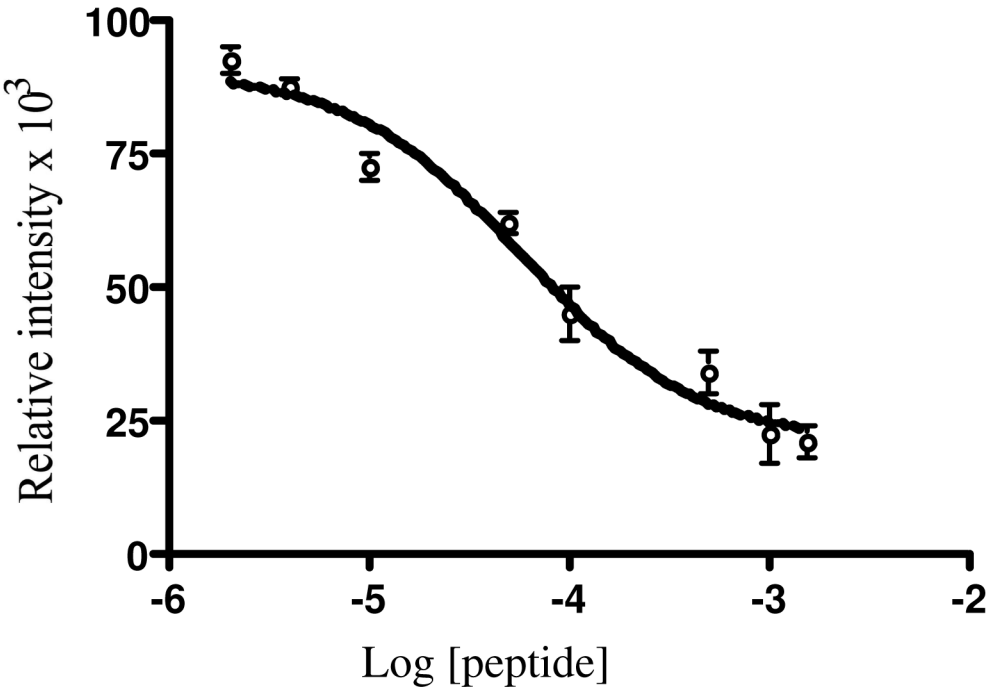


**Figure 7.**

Plot of relative intensity *vs*. Log [**1**] to determine the $IC_{50}$ of the peptide binding to α2. Measurements were carried out at 22±1°C in 50 mM HEPES, 15 mM $MgSO_4$, 1 mM EDTA, pH 7.6. Error bars are the standard deviation of three independent measurements.

**Table 1**

$K_d$s for the interaction between DAN-β2 variants and α2 determined by fluorescence titration[a]

| DAN-β2 variants | $K_d$ |
|---|---|
| DAN-β2(V351C) | 0.38±0.06 |
| DAN-β2(Y356C) | 0.41±0.06 |
| DAN-β2(V365C) | 0.36±0.07 |
| DAN-β2(T367C) | 0.34±0.07 |

[a]Conditions: 50 mM HEPES, 15 mM $MgSO_4$, 1 mM EDTA, pH 7.6 at 22±1°C.

**Table 2**

Specific activities of β2 variants.

| Proteins | Cys Variants nmol/mg/min | BP Variants nmol/mg/min | DAN Variants nmol/mg/min |
|---|---|---|---|
| β2(S341) | - | 3.4 | - |
| β2(N343) | 1210 | 893.7 | - |
| β2(Q345) | - | 8.8 | - |
| β2(A347) | - | 8.4 | - |
| β2(Q349) | - | 4.7 | - |
| β2(V351) | - | 74 | - |
| β2(V353) | 300 | 28 | - |
| β2(Y356) | 11 | 4 | 6.8 |
| β2(V358) | - | 43 | - |
| β2(I361) | 1091 | 161 | 533 |
| β2(V365) | 1575 | 158 | 540 |
| β2(T367) | 2586 | 482 | 601 |
| β2(L370) | - | 209 | - |
| β2(F373) | 1168 | 1093 | - |
| β2(L375) | - | 297 | - |

For comparison, wt-β2 has an activity of 5933.0 nmol/mg/min. '-' denotes not determined. The lower limit of activity detection is 0.6 nmol/min/mg.